

Optical properties of a two-dimensional electron gas at even-denominator filling fractions

Darren J.T. Leonard¹, Neil F. Johnson¹, V. Nikos Nicopoulos¹ and F.J. Rodriguez²

¹ *Department of Physics, Clarendon Laboratory, Oxford University, Oxford OX1 3PU, England*

² *Departamento de Fisica, Universidad de Los Andes, Bogota A.A. 4976, Colombia*

Abstract

The optical properties of an electron gas in a magnetic field at filling fractions $\nu = \frac{1}{2m}$ ($m = 1, 2, 3 \dots$) are investigated using the composite fermion picture. The response of the system to the presence of valence-band holes is calculated. The shapes of the emission spectra are found to differ qualitatively from the well-known electron-hole results at zero magnetic field. In particular, the asymmetry of the emission lineshape is found to be sensitive to the hole-composite fermion plane separation.

PACS numbers: 71.10.Pm, 73.40.Hm, 78.55.-m, 78.66.-w

I. INTRODUCTION

Recent theoretical studies of the properties of a two-dimensional electron gas at filling factor $\nu = \frac{1}{2m}$ [1,2] have shown that the system of electrons at finite magnetic field can be mapped on to one of new quasi-particles, composite fermions (CFs), which do not experience any magnetic field. An additional bonus of this mapping is that the resulting CFs have weak interactions, even though the original electrons were strongly interacting. These remarkable results are obtained by applying a singular gauge transformation to the electron system; this transformation has the effect of attaching $2m$ quanta of magnetic flux to each electron. At the mean field level, the ground state of the system is now one of a Fermi liquid of CFs. Studies have centred on the transport properties of the CF gas – to our knowledge no work has yet been published regarding its optical properties. This is in spite of recent experiments which optically probe the two-dimensional electron gas in the Fractional Quantum Hall regime around $\nu = \frac{1}{2}$ (e.g. Refs. [3] and [4]).

The purpose of this paper is to investigate the optical signature of a CF gas at even denominator filling fractions $\nu = \frac{1}{2m}$. The CFs in this paper are treated at the mean-field level only. As a consequence, the CFs are non-interacting particles [1,2]; this simplifies the treatment of the CF-hole interaction since there will be no dielectric screening by the CF gas. In the seminal paper of Halperin, Lee and Read [1], the response of the CF gas to impurity potentials is considered. The localized potential causes density fluctuations in the CF gas and consequently a fluctuation in the magnetic field. In the experimental heterostructures of Turberfield and co-workers [3], however, the valence-band hole is delocalized, i.e. the corresponding hole potential is not localized. Consequently we do not expect the effect of the induced vector potential to be so important. The valence hole can therefore be reasonably described as a weak (delocalized) probe with the interaction strength taken as a parameter dependent on the plane separation d . Within the mean-field approximation, therefore, the problem reduces to that of a gas of CFs, which experience no magnetic field, interacting with valence holes which feel the full $\nu = \frac{1}{2m}$ magnetic field (see Fig. 1). This feature makes

the problem different from the case of electrons and holes interacting at zero magnetic field. As we will show, this has an interesting effect on the shape of the optical spectra, which depends on the competition between the effects due to the dipole matrix elements and those due to the CF-hole interaction.

In accordance with the experimental GaAlAs heterostructure systems containing delocalized holes [3,4], our model considers CFs and holes constrained to parallel planes separated by a distance d . The CF-hole interaction depends on this separation and as a result the optical properties are altered by a change of d . The treatment of many-body optical effects presented here does not address some of the more subtle issues concerning hole self-energies that have been discussed recently in connection with Fermi-edge enhancement effects in the two-dimensional electron gas. However, the simplifications employed here do allow a number of analytic results to be obtained, thereby reducing the build-up of numerical errors. The general qualitative features obtained here should also arise in a fuller treatment. It is known that the hole self-energy diagrams contribute greatly to the suppression of the Mahan exciton into a Fermi-edge singularity as a result of the orthogonality catastrophe [5–9]. This effect is crudely taken into account here via the broadening of the hole spectral function from a delta-function to a Lorentzian. The form employed here permits an *analytic* calculation of the zero-order CF-dressed-hole Green function at finite temperature; this function represents the building block for a ladder-approximation treatment of CF-hole interactions.

The plan of the paper is as follows. In Sec. II, we review the relevant single-particle results. Section III provides the formal expressions used in the calculation of the optical properties; in particular, the dielectric function (III.A), the dipole matrix elements (III.B) and the CF-hole Green function (III.C and III.D). Specific optical spectra are discussed in Sec. IV at half-filling, with Sec. V providing the conclusions.

II. SINGLE PARTICLE PROPERTIES

A. Composite Fermions

The construction of the composite fermions (CFs) [1,2,10] from the conduction band electrons at $\nu = \frac{1}{2m}$ is achieved by making a gauge transformation which attaches $2m$ magnetic flux quanta to each electron. At the mean field-level this cancels out the externally applied magnetic field and screens completely the interaction between the particles. In the picture of CFs presented by Jain [11,10], the many-electron wavefunction of interacting electrons in a magnetic field is constructed from the wavefunction of non-interacting particles in a smaller magnetic field by attaching vortices to each particle, thereby introducing zeroes into the wavefunction. The vortices have the property of keeping the particles apart from each other, thereby modelling the effect of the repulsive interaction, and also of decreasing the filling factor. The net result is that the original interacting electron system at even denominator filling fractions is mapped on to the non-interacting CF system at zero effective magnetic field (c.f. Fig. 1).

At even denominator filling fractions the CF wavefunctions, normalised to an area L^2 , are taken to be

$$\Phi(\mathbf{r}) = \frac{1}{L} e^{i\mathbf{K} \cdot \mathbf{r}} \quad (1)$$

with energy $E \equiv \hbar\omega(\mathbf{K}) = \frac{\hbar^2\mathbf{K}^2}{2m_{CF}^*} + E_{gap}$; \mathbf{r} and \mathbf{K} are the two-dimensional position and momentum vectors respectively. CF creation and annihilation operators $c_{\mathbf{K}}^\dagger$ and $c_{\mathbf{K}}$ satisfy anticommutation relations $\{c_{\mathbf{K}}, c_{\mathbf{K}'}^\dagger\} = \delta_{\mathbf{K},\mathbf{K}'}$. Ignoring the fluctuations of the gauge field and assuming the CFs form a Fermi liquid with a renormalized effective *optical* mass m_{CF}^* , one may write the CF spectral function as $A_{CF}(\mathbf{K}, \omega) = 2\pi\delta(\omega(\mathbf{K}) - \omega)$. The CF chemical potential must be determined by the fact that the system is at filling factor $\nu = \frac{1}{2m}$. Since for spinless particles in two dimensions the number density n is related to the Fermi wave vector by $4\pi n = k_f^2$, and related to the filling factor by $\nu = 2\pi l_o^2 n$, then at $\nu = \frac{1}{2m}$ one sees that $k_f = \frac{1}{l_0\sqrt{m}}$.

B. Hole States

The valence band holes (Fig. 1) are taken to have a single particle hamiltonian

$$H = \frac{(\mathbf{P} - e\mathbf{A})^2}{2m_h^*} . \quad (2)$$

Choosing the Landau gauge with $\mathbf{A} = Bx\mathbf{j}$ leads to states described by a Landau level index n and a y-momentum k

$$\Psi(x, y) = \frac{1}{\sqrt{2^n n! \sqrt{\pi} l_0 L}} e^{iky} H_n\left(\frac{x - kl_0^2}{l_0}\right) e^{-\frac{1}{2}(\frac{x - kl_0^2}{l_0})^2} \quad (3)$$

which have energy $E = \hbar\omega_c(n + \frac{1}{2})$ with $\omega_c = \frac{eB}{m_h^*}$ and $l_0^2 = \frac{\hbar}{m_h^* \omega_c}$, the functions $H_n(x)$ being the Hermite polynomials. An extremely important many-body effect governing the optical properties is that the hole states $|n, k\rangle$ can scatter from the low-energy CF excitations at the Fermi level. This results in a self-energy which can be written as a Lorentzian spectral function. One can crudely, but effectively, model this effect by approximating the spectral function as

$$A_h(k, \omega) = \frac{2\gamma}{(\omega - \frac{1}{2}\omega_c)^2 + \gamma^2} \quad (4)$$

where typically $\gamma \sim 10^{-2} \omega_c$. The hole creation and annihilation operators satisfy the anticommutation relations $\{d_{n,k_h}, d_{m,l_h}^\dagger\} = \delta_{n,m} \delta_{k_h, l_h}$. In this work the Landau level index is always zero and hence can be dropped.

III. OPTICAL RESPONSE

A. Dielectric Function

The optical response of a system to an external light field is characterized classically by the dielectric function, which gives the refractive index and an absorption coefficient [5,12,7]. Classically

$$\epsilon(\omega) = 1 + \chi(\omega) \quad (5)$$

where $\chi(\omega)$ is the susceptibility in the long-wavelength photon limit, and quantum mechanically

$$\chi(\omega) = -\frac{e^2}{\epsilon_0 V} R(\omega + i\delta) \quad R(\omega + i\delta) \equiv \langle\langle r(t); r(0) \rangle\rangle_{\omega+i\delta}^{irr} \quad (6)$$

Writing $\epsilon(\omega) = \epsilon_1(\omega) + i\epsilon_2(\omega)$, then the refractive index $n(\omega) = \sqrt{\frac{1}{2}(\epsilon_1(\omega) + (\epsilon_1(\omega)^2 + \epsilon_2(\omega)^2)^{\frac{1}{2}})}$ and the absorption coefficient $A(\omega) = \frac{\omega \epsilon_2(\omega)}{c n(\omega)}$. It is common practice to take $A(\omega) \propto \epsilon_2(\omega)$ close to the band gap, however this is an approximation since there can be an appreciable dependence of $n(\omega)$ on ω in this region. In order to calculate $A(\omega)$ one must have exact details of the system studied such as the size and the dipole matrix elements linking the valence and conduction band Bloch states. Typically the actual function plotted is just proportional to $\epsilon_2(\omega)$. In the region of the spectrum where $\epsilon_2(\omega)$ is negative, one has net optical gain since $A(\omega) < 0$; we label this as the emission spectrum. Similarly we label the region where $A(\omega) > 0$ to be the absorption spectrum.

B. Dipole Matrix Elements

The dipole operator correlation function in Eq. (6) is expanded in the CF-hole basis and reduces to

$$R(\omega + i\delta) = \sum_{\mathbf{K}, k, \mathbf{K}', k'} r_{cv}^*(\mathbf{K}, k) r_{cv}(\mathbf{K}', k') \left(G(k, \mathbf{K}; \mathbf{K}', k'; \omega + i\delta) + G(k, \mathbf{K}; \mathbf{K}', k'; -\omega - i\delta) \right) \quad (7)$$

where the two Green functions can be calculated using the usual Matsubara formalism assuming quasi-equilibrium conditions for the number density of particles. The CF states are labelled by the two-dimensional wavevector \mathbf{K} , whereas the hole states are labelled by a wavevector k in the y-direction. The interband matrix element in the envelope approximation for a transition from the hole state $|0, k\rangle$ to the conduction band state $|\mathbf{K}\rangle$ is given by

$$r_{cv}(\mathbf{K}, k) = r_{cv} \delta_{-k, K_y} \sqrt{\frac{2l_0\sqrt{\pi}}{L}} S(\mathbf{K}) \quad S(\mathbf{K}) \equiv e^{-iK_x K_y l_0^2 - \frac{1}{2}(K_x l_0)^2} \quad (8)$$

where r_{cv} is the matrix element of \hat{r} between the valence and conduction band Bloch states, assumed to be independent of \mathbf{K} . The novel feature of the present matrix elements, as compared with those obtained for the well-known situation of plane-wave valence and conduction states, is that there is only conservation of momentum in the y-direction; the damping of the matrix element in K_x is exponential and leads to a damping in the optical emission spectrum.

C. CF-Hole Green Function

1. Notation

The procedure to determine the optical response is now to calculate the Green function

$$G(k, \mathbf{K}; \mathbf{K}', k'; i\omega_n) \equiv - \int_0^\beta d\tau e^{i\omega_n \tau} \langle\langle T d_k(\tau) c_{\mathbf{K}}(\tau); c_{\mathbf{K}'}^\dagger d_{k'}^\dagger \rangle\rangle \quad (9)$$

in a perturbation expansion [5,7]. Due to the presence of the y-momentum-conserving terms in the dipole correlation function, the hole wavevector $k = -K_y$, where K_y is the CF y-wavevector. Thus the Green functions are dependent on only four labels i.e. the four components of \mathbf{K} and \mathbf{K}' . Hence the notation for the Green function to be calculated can be simplified by defining

$$G(\mathbf{K}; \mathbf{K}'; \xi) \equiv G(-K_y, \mathbf{K}; \mathbf{K}', -K'_y; \xi) \quad G(\mathbf{K}; \xi) \equiv G(\mathbf{K}; \mathbf{K}; \xi). \quad (10)$$

Defining

$$\Pi(\xi) = \sum_{\mathbf{K}, \mathbf{K}'} S^*(\mathbf{K}) S(\mathbf{K}') G(\mathbf{K}, \mathbf{K}'; \xi) \quad (11)$$

one can write

$$A(\omega) \propto -\text{Im } B(\omega) \quad B(\omega) \equiv \Pi(\omega + i\delta) + \Pi(-\omega - i\delta). \quad (12)$$

2. Perturbation Expansion of $G(\mathbf{K}; \mathbf{K}'; i\omega)$

The perturbation to be introduced is the interaction between CFs and holes. CFs and holes have equal and opposite charges; a natural assumption for the interaction form might be an unscreened Coulomb potential which conserves y-momentum. The nature of the wavefunctions implies that the form of the subsequent potential matrix elements is peculiar to the system,

$$V(\mathbf{K}, k, k', \mathbf{K}') = -\frac{e^2}{\epsilon_0 \epsilon_r} \frac{e^{-|\mathbf{K} - \mathbf{K}'|d}}{|\mathbf{K} - \mathbf{K}'|} e^{-\frac{1}{4}l_0^2|\mathbf{K} - \mathbf{K}'|^2 - \frac{i}{2}l_0^2(K_x - K'_x)(k + k')} \quad (13)$$

where $\epsilon_r \approx 13$ is the bulk GaAlAs dielectric constant, and d is the CF-hole separation in the direction perpendicular to the CF plane. Unfortunately the complexity of these matrix elements makes subsequent analysis extremely difficult, even numerically. Our approach will therefore center on the use of a constant (i.e. momentum-independent) matrix element V_0 which allows one to sum the diagrammatic expansion of the Green function in the ladder diagram approximation easily, and yet still retains the essential qualitative features of the true interaction [5,6]. This produces a simple analytical expression for the Green function in terms of integrations over \mathbf{K} of the zero-order CF-hole Green function. Poles of the Green function indicating possible bound states, which leads to the observation of excitonic effects such as the Fermi-edge singularity, are then easy to find. In order to choose an appropriate value for V_0 , we set the momentum transfer in Eq. (13) to be $|\mathbf{K} - \mathbf{K}'| \sim k_f = \frac{1}{l_0 \sqrt{m}}$ i.e. typical for scattering across the Fermi surface; we also ignore the final oscillatory term in Eq. (13). The resulting matrix element V_0 is then seen to scale with d like $e^{-k_f d}$. The inter-plane separation is therefore a parameter which can be used to scale the value of the potential V_0 . Spectra can be generated for different values of the scaling factor $e^{-k_f d}$, hence the effect on the spectrum of different ratios $\frac{d}{l_0 \sqrt{m}}$ can be determined.

The diagrammatic expansion of $G(\mathbf{K}; \mathbf{K}'; i\omega)$ (see Fig. 2) in this approximation becomes

$$G(\mathbf{K}; \mathbf{K}'; i\omega) = G_0(\mathbf{K}; i\omega) \delta_{\mathbf{K}, \mathbf{K}'} + \frac{G_0(\mathbf{K}; i\omega) V_0 G_0(\mathbf{K}'; i\omega)}{1 - V_0 \sum_{\mathbf{K}''} G_0(\mathbf{K}''; i\omega)} \quad (14)$$

where the zero-order CF-hole propagator is $G_0(\mathbf{K}; i\omega)$. Hence from Eq. (11)

$$\Pi(i\omega) = \sum_{\mathbf{K}} |S(\mathbf{K})|^2 G_0(\mathbf{K}; i\omega) + \frac{V_0 \sum_{\mathbf{K}} S^*(\mathbf{K}) G_0(\mathbf{K}; i\omega) \sum_{\mathbf{K}'} S(\mathbf{K}') G_0(\mathbf{K}'; i\omega)}{1 - V_0 \sum_{\mathbf{K}''} G_0(\mathbf{K}''; i\omega)} \quad (15)$$

is the basis of the calculation of the optical response. Analytically continuing $i\omega \rightarrow \omega + i\delta$ and $-\omega - i\delta$ generates the correct functions $\Pi(\omega + i\delta)$ and $\Pi(-\omega - i\delta)$ from which $B(\omega)$ results. However it is only necessary to calculate $\Pi(\omega + i\delta)$ which is the ‘resonant’ term, not $\Pi(-\omega - i\delta)$, for the study of the optical response [7]. Since the matrix elements are an important quantity in determining the shape of the spectra, it will also be interesting to examine the spectra when the matrix elements are constant over \mathbf{K} , i.e. $S(\mathbf{K}) = 1$. This results in

$$\Pi'(i\omega) = \sum_{\mathbf{K}} G_0(\mathbf{K}; i\omega) + \frac{V_0 \sum_{\mathbf{K}} G_0(\mathbf{K}; i\omega) \sum_{\mathbf{K}'} G_0(\mathbf{K}'; i\omega)}{1 - V_0 \sum_{\mathbf{K}''} G_0(\mathbf{K}''; i\omega)} \quad (16)$$

D. Zero-Order CF-Hole Propagator

The zero-order CF-hole propagator $G_0(\mathbf{K}, i\omega)$ can be written in the spectral representation [5–7] as

$$G_0(\mathbf{K}; i\omega_n) = \int_{-\infty}^{\infty} \frac{d\omega_1}{2\pi} \int_{-\infty}^{\infty} \frac{d\omega_2}{2\pi} \frac{A_{CF}(\mathbf{K}, \omega_1) A_h(-K_y, \omega_2) [1 - f(\omega_1 - \frac{\mu_{CF}}{\hbar}) - f(\omega_2 - \frac{\mu_h}{\hbar})]}{i\omega_n - \hbar\omega_1 - \hbar\omega_2}. \quad (17)$$

The function $f(\omega) = (e^{\beta\hbar\omega} + 1)^{-1}$ is a Fermi-Dirac distribution factor for the number of particles at a given energy; μ_{CF} and μ_h are the chemical potentials for the CFs and holes respectively. Making a change of variables to $x = \frac{1}{2}\mathbf{K}^2 l_0^2$ and $\Omega = \omega - \omega_g - \frac{1}{2}\omega_c$ and with $\mu_h = \hbar(\frac{1}{2}\omega_c - \omega_\Delta)$, we obtain

$$\begin{aligned} \hbar G_0(x, \Omega + i\delta) [(\Omega - \omega_c^* x)^2 + \gamma^2] &= [1 - f(\omega_c^*(x - \frac{1}{2m})) - f(\omega_\Delta + i\gamma)] (\Omega - \omega_c^* x) \\ &\quad - i\gamma [\frac{1}{2} - f(\omega_c^*(x - \frac{1}{2m})) + f(\omega_\Delta + i\gamma) - f(\Omega - \omega_c^* x + \omega_\Delta)] \\ &\quad + \frac{\gamma}{\pi} \text{Re}[\psi(\frac{1}{2} - \frac{i\beta\hbar}{2\pi}(\Omega - \omega_c^* x + \omega_\Delta))] \\ &\quad + \frac{i}{2\pi} [(\Omega - \omega_c^* x + i\gamma) \psi(\frac{1}{2} - \frac{\beta\hbar}{2\pi}(\gamma - i\omega_\Delta)) - (\Omega - \omega_c^* x - i\gamma) \psi(\frac{1}{2} + \frac{\beta\hbar}{2\pi}(\gamma + i\omega_\Delta))] \end{aligned} \quad (18)$$

where the Digamma function $\psi(z)$ is defined as

$$\psi(z) \equiv -C - \sum_{n=0}^{\infty} \left(\frac{1}{z+n} - \frac{1}{1+n} \right) \quad (19)$$

with C being Euler's constant. In terms of $G_0(x, \Omega + i\delta)$ and $W = -\frac{V_0}{2\pi\hbar\omega_c l_0^2}$, which is the ratio of the Coulomb energy to the kinetic cyclotron energy, we obtain

$$\begin{aligned} \Pi(\Omega + i\delta) = & \quad (20) \\ & \frac{1}{2\pi\hbar\omega_c l_0^2} \left[\int_0^\phi dx e^{-x} I_0(x) \hbar\omega_c G_0(x, \Omega + i\delta) - \frac{W \left(\int_0^\phi dx e^{-\frac{1}{2}x} J_0\left(\frac{\sqrt{3}}{2}x\right) \hbar\omega_c G_0(x, \Omega + i\delta) \right)^2}{1 + W \int_0^\phi dx \hbar\omega_c G_0(x, \Omega + i\delta)} \right] \end{aligned}$$

where ϕ is a cut-off determined by the size of the Brillouin Zone associated with the bulk semiconductor environment. The Bessel functions $I_0(x)$ and $J_0(x)$ are defined as

$$I_0(x) \equiv \sum_{n=0}^{\infty} \frac{1}{(n!)^2} \left(\frac{x}{2} \right)^{2n} \quad J_0(x) \equiv \sum_{n=0}^{\infty} \frac{(-1)^n}{(n!)^2} \left(\frac{x}{2} \right)^{2n}. \quad (21)$$

We note that we have reduced the problem of calculating $\Pi(\Omega + i\delta)$ to a relatively straightforward one-dimensional integral over x . For the case of constant matrix element $S(\mathbf{K}) = 1$ the corresponding result is

$$\Pi'(\Omega + i\delta) = \frac{1}{2\pi\hbar\omega_c l_0^2} \left[\frac{\int_0^\phi dx \hbar\omega_c G_0(x, \Omega + i\delta)}{1 + W \int_0^\phi dx \hbar\omega_c G_0(x, \Omega + i\delta)} \right] \quad (22)$$

IV. RESULTS AT HALF FILLING

In this section the imaginary part of the dielectric function is calculated at $\nu = \frac{1}{2}$ for parameters taken in accordance with the GaAlAs heterostructure system studied in Ref. [3]. The areal density of electrons (CFs) is 10^{15} m^{-2} , the hole effective mass is taken as $0.45m_e$, and an electron and hole temperature of 0.1K is used. One further parameter is needed which is the CF effective mass. On the basis of the expectation that at $\nu = \frac{1}{2}$ the emission spectrum should occur over the Fermi surface, we can equate the width of the peak observed in experiments in Ref. [3] to the Fermi energy $E_f = \frac{1}{2}\hbar\omega_c^*$; the particular data used implies $m_{CF}^* = 0.70m_e$ with $\omega_c^* = 0.64\omega_c$. The chemical potential of the holes is set so that the hole

number density is small compared to the number of CFs, and yet there is still a measurable emission spectrum; we use $\omega_\Delta = 0.02\omega_c$ which gives $\frac{n_h}{n_{CF}} = 0.15$. The spectra are plotted against a photon energy $\hbar\Omega$ in units of the Fermi energy.

Enhancements of the optical properties of the CFs occur as a result of the attractive interaction between the CFs and the holes, which try to form CF-excitons. It is clear from Eq. (21) that there is an excitonic enhancement of the optical response when

$$1 + W \int_0^\phi dx \hbar\omega_c \operatorname{Re} G_0(x, \Omega + i\delta) = 0 . \quad (23)$$

The frequencies for which this is true are the Mahan exciton states [5], these being the equivalent of the two-particle exciton states when there is a large number density of CFs. These excitonic states only form when the potential is sufficiently strong to bind up CFs and holes. Since the strength of the potential is determined by the separation of the CF and hole planes d , then the separation is crucial in deciding the strength of enhancement and hence the lineshape of the optical spectra. Figure 3 shows the real and imaginary parts of $\int_0^\phi dx \hbar\omega_c G_0(x, \Omega + i\delta)$; it also shows plots of $-\frac{1}{W}$ (dashed lines) which arise from different d as indicated, and condition (23) is satisfied when these dashed lines cross the solid curve, with the Mahan exciton frequencies being the points of intersection. As can be seen from the figure, the potentials used here are *not* strong enough to create bound Mahan excitons; however it is clear from the plots of the imaginary part of the dielectric function that the interaction enhances the spectra at the Fermi surface due to the increasing overlap of CFs and holes, even if the potential is not strong enough to bind them up.

Figure 4 shows the emission part of the spectrum for CFs and holes separated by various inter-plane distances d . We note that the dipole matrix elements will, in principle, also be dependent on the overlap of the parts of the CF and hole wavefunctions which lie in the ‘z’ direction, i.e. perpendicular to the planes; however these will mostly affect the *intensities* of the spectra but *not the lineshapes*. We are only interested in the variation of the lineshape with the separation d . The curve showing emission when there is no interaction, exhibits an intrinsic asymmetry in the lineshape with a *left bias*; this results purely from the dipole

matrix elements and hence $S(\mathbf{K})$. As a comparison, Fig. 5 shows the emission when this factor is taken to be constant, i.e. from Eq. (22). Figures 4 and 5 illustrate the difference that the CF-hole matrix element has on the lineshape. One can also make comparisons between the intensities for lines with the same d ; it is noticeable that the emission intensity is reduced by the inclusion of the correct factor $S(\mathbf{K})$. Switching on the interaction changes the asymmetry from *left* to *right* as d is decreased; this results from enhancement appearing at the Fermi surface which is essentially of logarithmic-divergence character [5]. The interaction potential has not been allowed to be strong enough to cause the Mahan exciton to bind, i.e. Eq. (23) is never satisfied. This is because such a singularity is always suppressed in practice by the orthogonality catastrophe [5,6,8] into a straightforward Fermi-edge enhancement. The results shown in Fig. 4 can also be applied to other even-denominator fractions $\nu = \frac{1}{2m}$, after a simple rescaling of ω_c^* . Interestingly, the predicted asymmetry in the emission lineshape (see Fig. 4) seems consistent with recent photoemission experiments [4], where either a left or right-biased lineshape can be observed according to the specific heterostructure sample and fraction $\frac{1}{2m}$ being studied, i.e. according to the magnitude of $\frac{d}{l_0}$. A detailed comparison with this experimental data will be presented in a future publication [13].

Figures 6 and 7 show the absorption part of the spectra. As with Figs. 4 and 5, Fig. 6 is calculated including the correct factor $S(\mathbf{K})$ while Fig. 7 has this factor set to unity. The effect of the \mathbf{K} -dependence is not as clear here as it is in emission, but it is still evident. Consider the spectra when the interaction is turned off; in Fig. 7 the curve is constant above about $1.2E_f$, being consistent with the step function associated with absorption at zero temperature and with no hole broadening [5]. However there is a decay at higher energies in Fig. 6 associated with the factor $e^{-x}I_0(x)$ in Eq. (21) resulting directly from the matrix element factor $S(\mathbf{K})$. When the interaction is turned on, one observes the enhancement at the Fermi-edge resulting from the tendency to form Mahan excitons, with the spectra in Fig. 6 being smaller in amplitude than in Fig. 7, again as a result of the \mathbf{K} -dependence of the matrix element.

V. CONCLUSION

This paper has calculated the optical signature of a composite fermion (CF)-hole system at even-denominator filling fractions $\nu = \frac{1}{2m}$. The shapes of the emission and absorption spectra have been found to differ from the well-known electron-hole results at zero magnetic field. The results suggest that emission lineshapes measured in photoluminescence experiments on GaAlAs heterostructures at $\nu = \frac{1}{2m}$ can be used to extract information concerning the electron-hole plane separation. Future work will focus upon including effects of gauge fluctuations (i.e. effective CF-CF interactions) into the formalism; of particular interest is the question of how such gauge fluctuations will affect the optical spectra.

Acknowledgements We acknowledge the financial support of EPSRC through a Studentship (D.J.T.L), EPSRC Grant No. GR/K 15619 (N.F.J. and V.N.N.) and COLCIENCIAS (F.J.R.). We would like to thank Andrew Turberfield for very useful discussions. We are also grateful to Robin Nicholas, Henry Cheng, Taco Portengen and Luis Quiroga. We thank Henry Cheng for showing us his experimental data prior to publication.

REFERENCES

- [1] B.I. Halperin, P.A. Lee and N. Read, Phys. Rev. B **47**, 7312 (1993).
- [2] A. Stern and B.I. Halperin, Phys. Rev. B **52**, 5890 (1995).
- [3] I.N. Harris, H.D.M. Davies, R.A. Ford, J.F. Ryan, A.J. Turberfield, C.T. Foxon and J.J. Harris, Surf. Sci. **305**, 61 (1994); I.N. Harris, Oxford University, DPhil. Thesis, 1994; A.J. Turberfield (unpublished).
- [4] H.H. Cheng and R.J. Nicholas (unpublished).
- [5] G.D. Mahan, Many Particle Physics (Plenum, New York, 1981); Phys. Rev. **153**, 3882 (1967); Phys. Rev. **163**, 3612 (1967).
- [6] F.J. Rodriguez and C. Tejedor, Phys. Rev. B **47**, 1506 (1993); Phys. Rev. B **47**, 13015 (1993).
- [7] H. Haug and S. Schmitt-Rink, Prog. in Quant. Electr. **9**, 1 (1984).
- [8] P. Nozieres and C.T. de Dominicis, Phys. Rev. **178**, 1097 (1969).
- [9] A.E. Ruckenstein and S. Schmitt-Rink, Phys. Rev. B **35**, 7551 (1987).
- [10] J.K. Jain, Adv. in Phys. **41**, 105 (1992); Phys. Rev. Lett. **63**, 2199 (1989); Phys. Rev. B **41**, 7653 (1990).
- [11] E. Rezayi and N. Read, Phys. Rev. Lett. **72**, 6900 (1994); N. Read, Proceedings of the Eleventh International Conference on the *Electronic Properties of Two Dimensional Systems*, Nottingham (1995).
- [12] Hartmut Haug and Stephan W. Koch, Quantum Theory of the Optical and Electronic Properties of Semiconductors (World Scientific, 1990).
- [13] D.J.T. Leonard and H.H. Cheng, in preparation.

Figure Captions

Figure 1: Effective composite fermion (CF) and hole band structure diagram.

Figure 2: Diagrammatic expansion of $G(\mathbf{K}; \mathbf{K}'; i\omega)$ in the ladder approximation. The diagrams are closed by the dipole matrix elements, which conserve y-momentum; since this is just the photon momentum, the only diagrams required are those where the total y-momentum is zero.

Figure 3: Real and imaginary parts of the integrated CF-hole Green function (solid lines) together with plots of the inverse of the CF-hole interaction strengths $-\frac{1}{W}$ for different CF-hole plane separations d (dashed lines). The magnetic length l_0 is typically 89Å at $B = 8T$ with $\nu = \frac{1}{2}$ and $n_e = 10^{15} m^{-2}$. The Fermi energy $E_f = 0.7 meV$.

Figure 4: Emission spectrum (i.e. $A(\omega) < 0$) obtained from the imaginary part of the dielectric function, plotted with different plane separations d and with the full \mathbf{K} -dependent matrix elements. Input parameters correspond to GaAlAs heterostructure. The magnetic length l_0 is typically 89Å at $B = 8T$ with $\nu = \frac{1}{2}$ and $n_e = 10^{15} m^{-2}$. The Fermi energy $E_f = 0.7 meV$.

Figure 5: Emission spectrum (i.e. $A(\omega) < 0$) obtained from the imaginary part of the dielectric function, plotted with different plane separations d as in Fig. 4, but *without* \mathbf{K} -dependent matrix elements. Input parameters as in Fig. 4.

Figure 6: Absorption spectrum (i.e. $A(\omega) > 0$) obtained from the imaginary part of the dielectric function, plotted with different plane separations d and with full \mathbf{K} -dependent matrix elements. Input parameters correspond to Fig. 4.

Figure 7: Absorption spectrum (i.e. $A(\omega) > 0$) obtained from the imaginary part of the dielectric function, plotted with different plane separations d as in Fig. 6 but *without* \mathbf{K} -dependent matrix elements. Input parameters correspond to Fig. 4.

Figure 2. (Leonard, PRB)

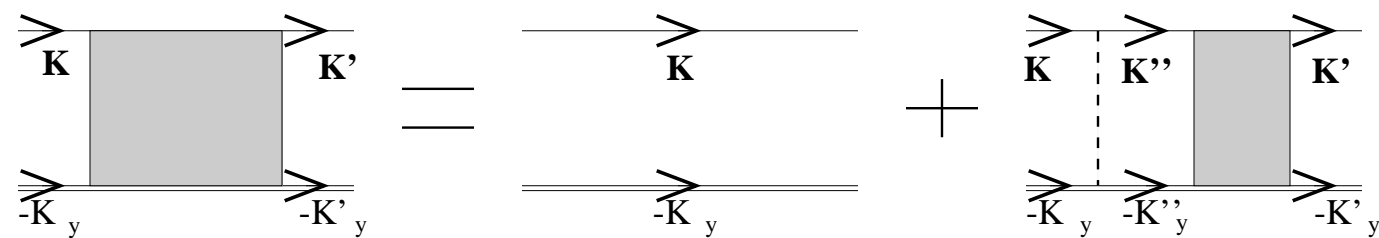


Figure 1. (Leonard, PRB)

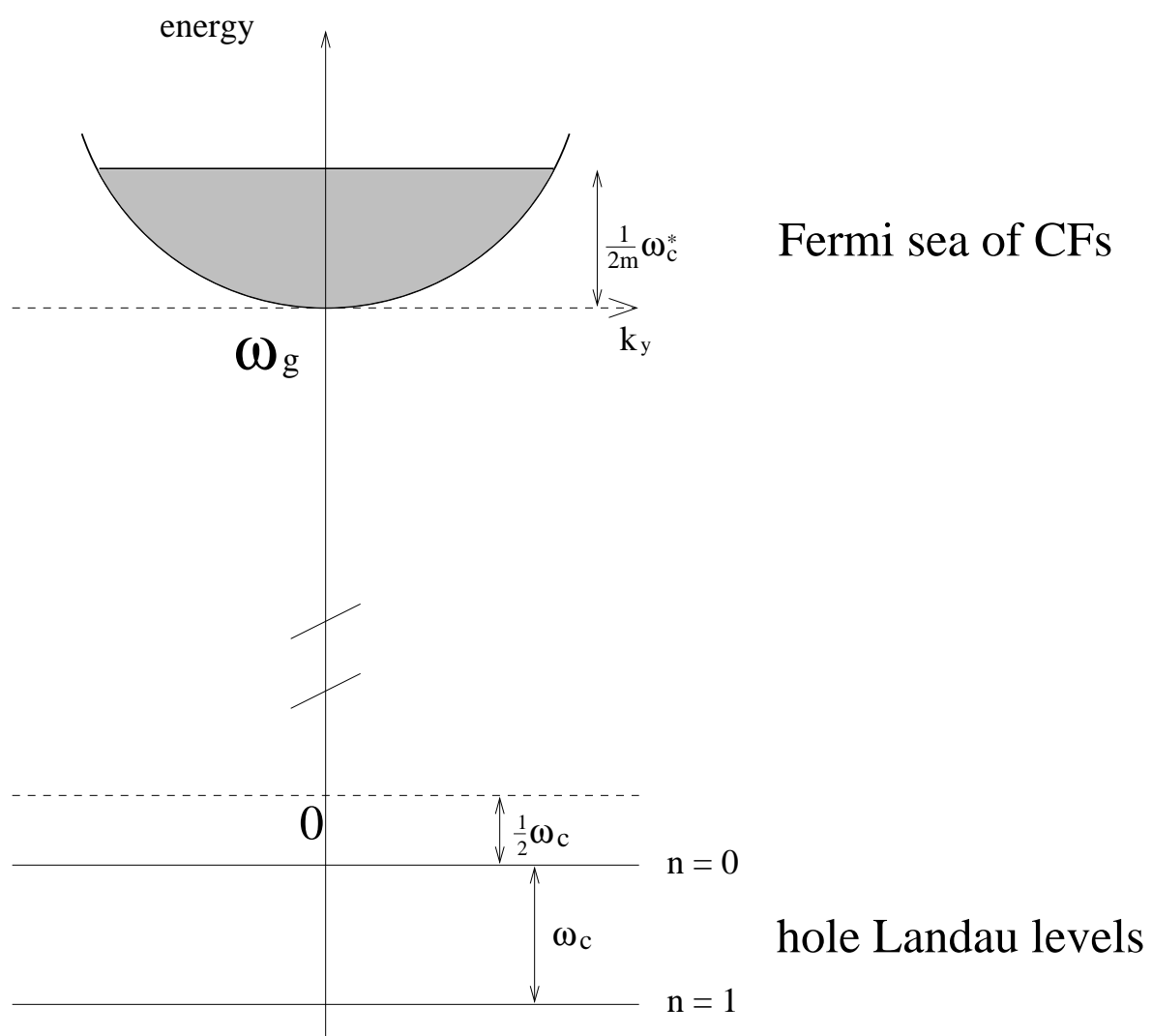


Figure 3. (Leonard, PRB)

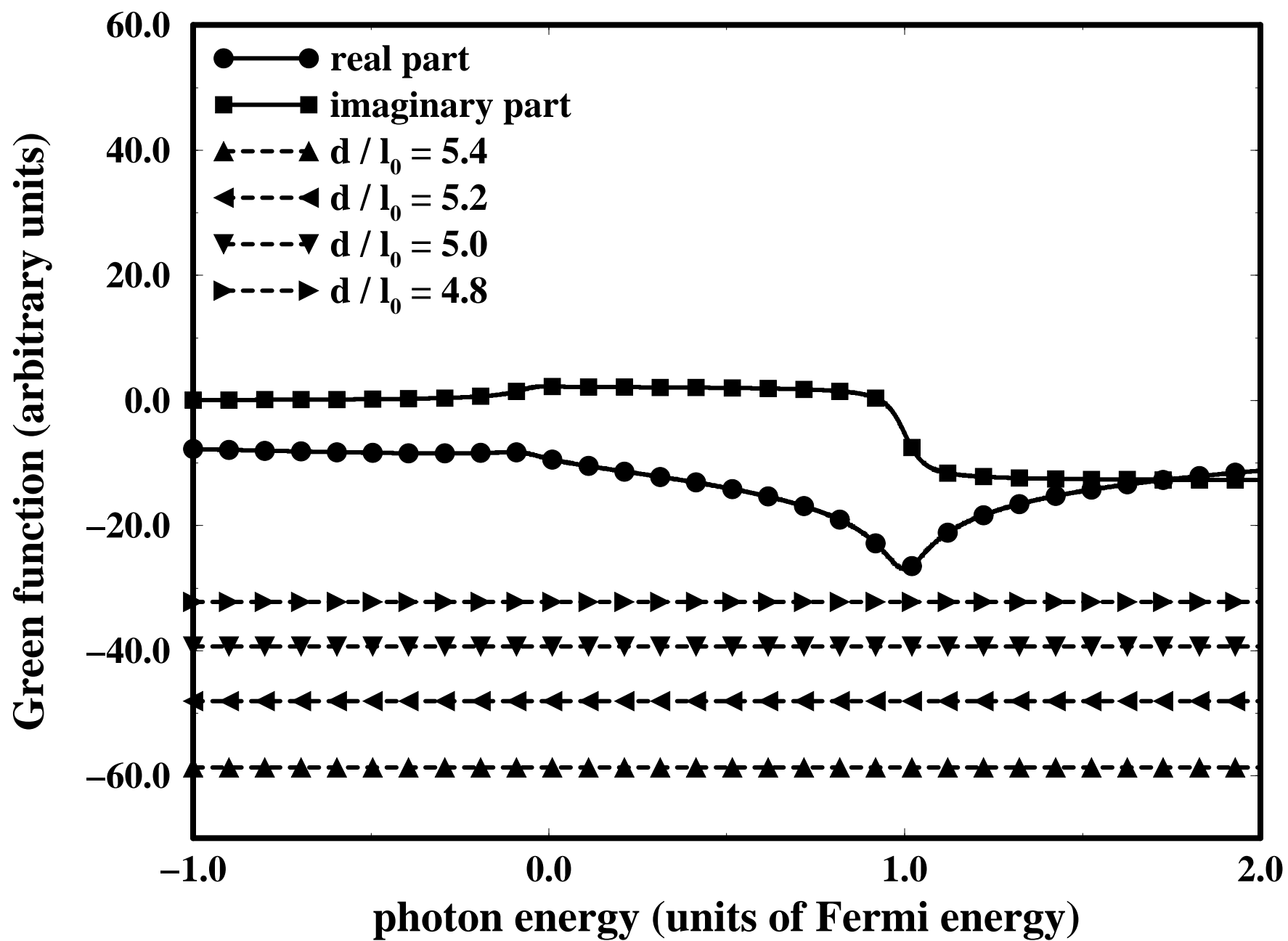


Figure 4. (Leonard, PRB)

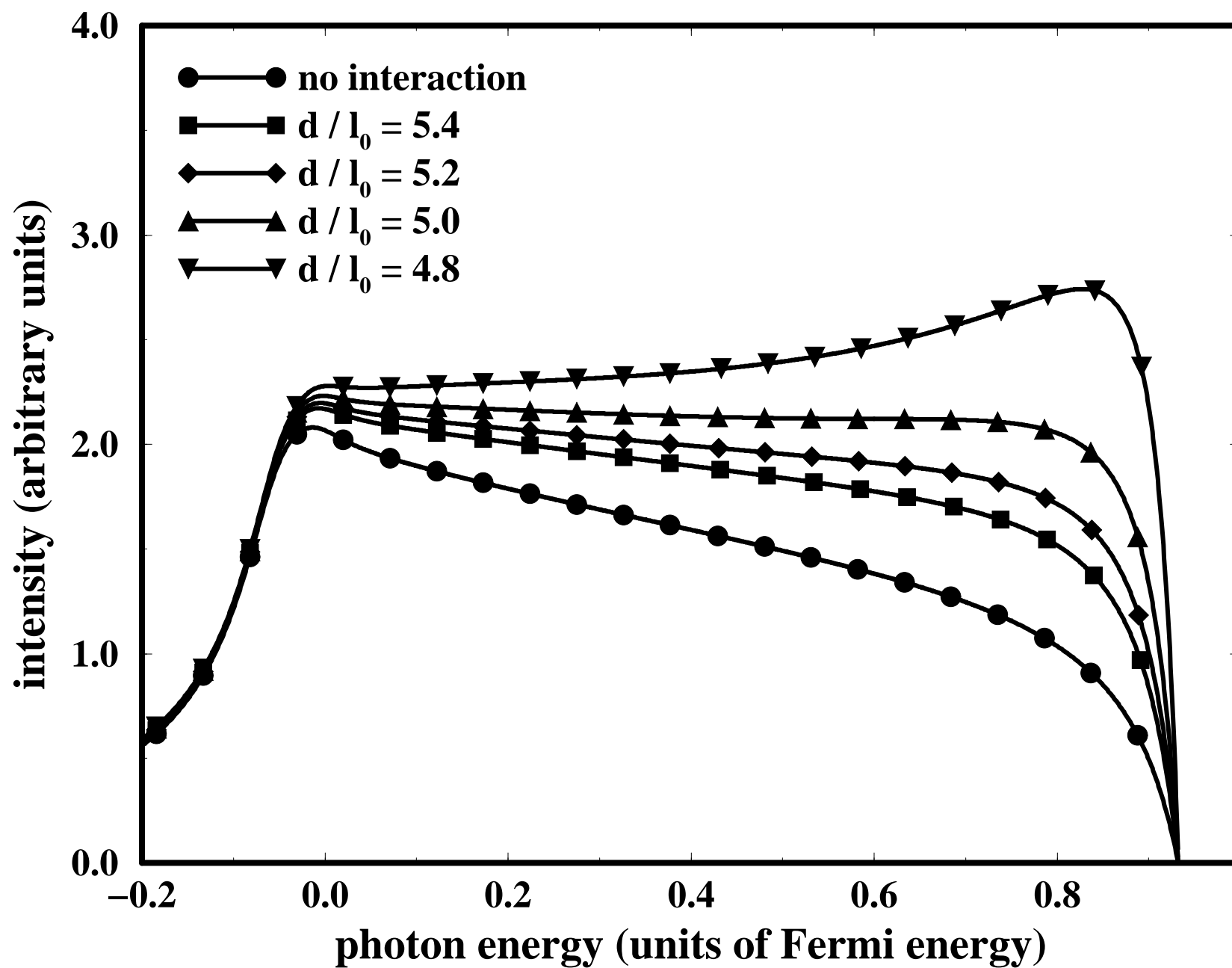


Figure 5. (Leonard, PRB)

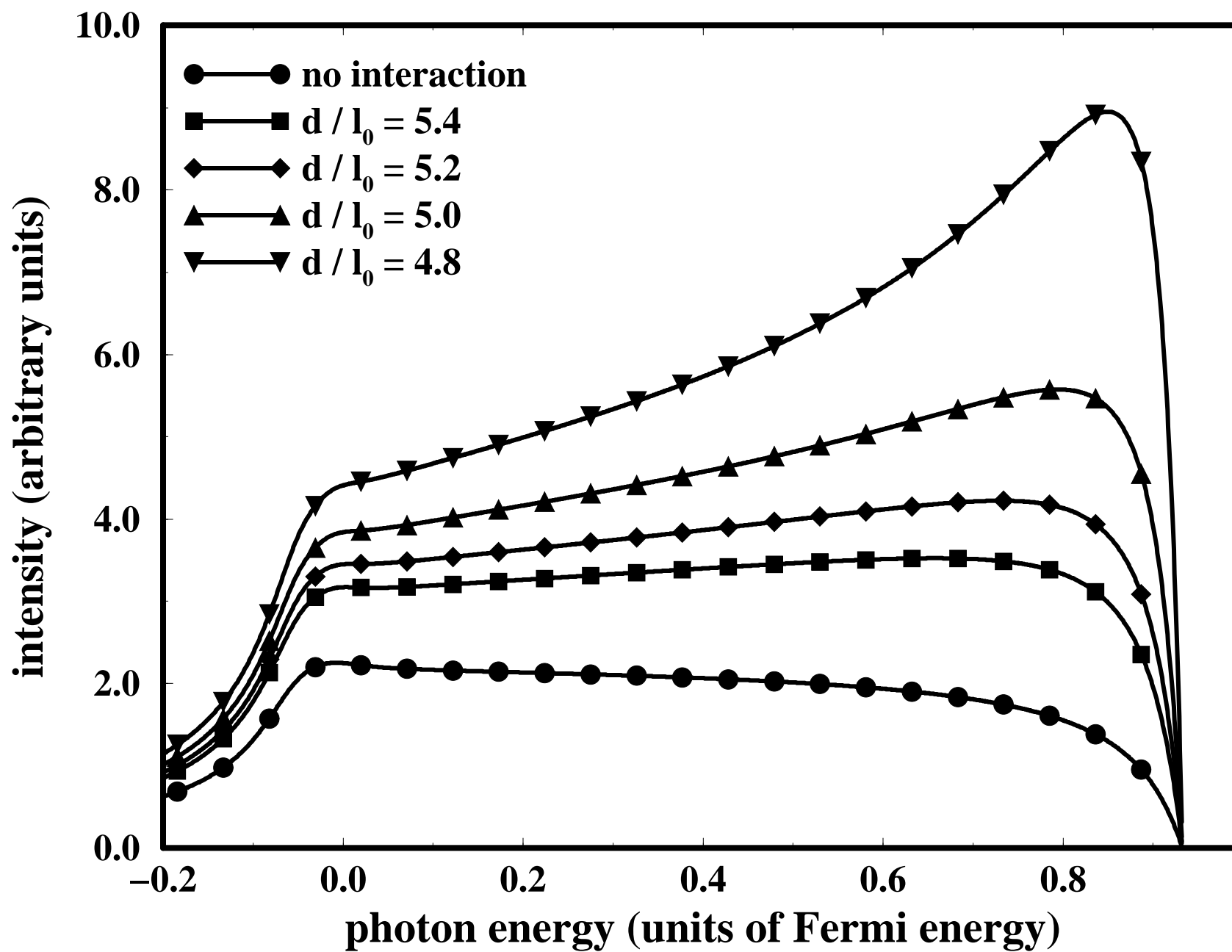


Figure 6. (Leonard, PRB)

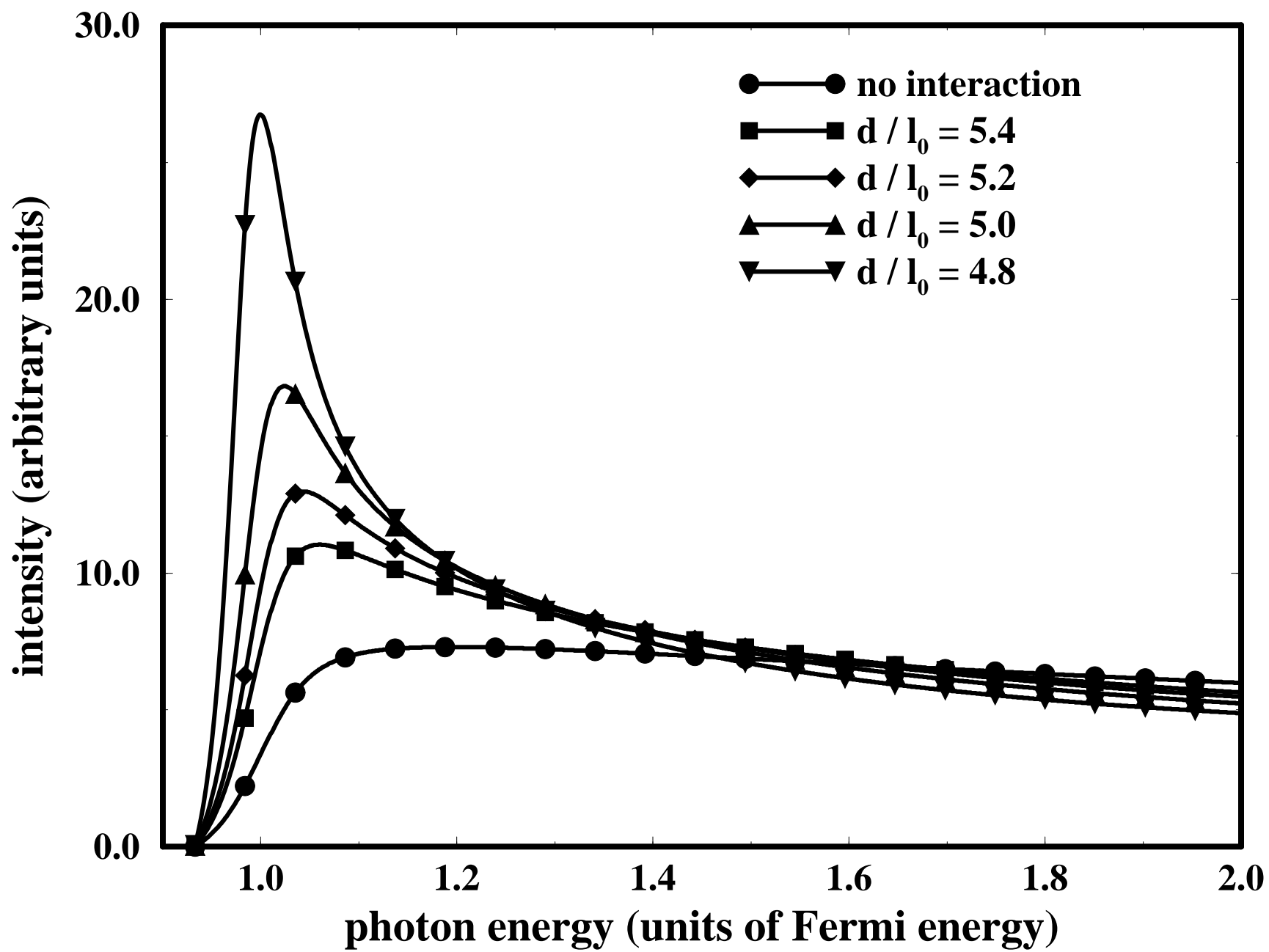


Figure 7. (Leonard, PRB)

